Materials Science and Engineering C 33 (2013) 4935–4943

Contents lists available at ScienceDirect

Materials Science and Engineering C

journal homepage: www.elsevier.com/locate/msec

Fabrication of novel nanofiber scaffolds from gum tragacanth/poly(vinyl alcohol) for wound dressing application: In vitro evaluation and antibacterial properties

Marziyeh Ranjbar-Mohammadi [a], S. Hajir Bahrami [a,*], M.T. Joghataei [b]

[a] Textile Engineering Department, Amirkabir University of Technology, Tehran, Iran
[b] Cellular and Molecular Research Center, Tehran University of Medical Science, Tehran, Iran

ARTICLE INFO

Article history:
Received 21 April 2013
Received in revised form 1 July 2013
Accepted 13 August 2013
Available online 28 August 2013

Keywords:
Electrospinning
Nanofiber
Gum tragacanth
Antibacterial

ABSTRACT

Gum tragacanth (GT) is one of the most widely used natural gums which has found applications in many areas because of its attractive features such as biodegradability, nontoxic nature, natural availability, higher resistance to microbial attacks and long shelf-life properties. GT and poly(vinyl alcohol) (PVA) were dissolved in deionized water in different ratios i.e., 0/100, 30/70, 60/40, 50/50, 40/60, 70/30, 0/100 mass ratio of GT/PVA. Nanofibers were produced from these solutions using electrospinning technique. The effect of different electrospinning parameters such as extrusion rate of polymer solutions, solution concentration, electrode spacing distance and applied voltage on the morphology of nanofibers was examined. The antibacterial activity of nanofibers and GT solution against *Staphylococcus aureus* and *Pseudomonas aeruginosa* was examined and these nanofibers showed good antibacterial property against Gram-negative bacteria. FTIR data showed that these two polymers may be having hydrogen bonding interactions. DSC data revealed that the exothermic peak at about 194 °C for PVA shifted to a lower temperature in GT/PVA blend. Human fibroblast cells adhered and proliferated well on the GT/PVA nanofiber scaffolds. MTT assay was carried out on the GT/PVA nanofiber to investigate the proliferation rate of fibroblast cells on the scaffolds.

1. Introduction

Electrospinning is an interdisciplinary method to process solutions or melts, mainly from polymers, into long and continuous fibers with diameters ranging from tens of micrometers to tens of nanometers using an electrostatically driven jet [1]. Electrospinning appears to be simple, but is rather an intricate process that depends on different parameters such as molecular, process and technical variables. Depending on the polymer solution properties, equipment and processing variables, nanofibers produced have unique properties such as high surface to volume ratio, high porosity with upward interconnectivity which makes them suitable for transportation of nutrient, waste and cell communication in their different applications [2]. So far, hundreds of polymers from different sources have been directly electrospun into nanofibers using electrospinning technique [3–5]. Plant gums consisting of polysaccharides, are exuded from many trees and plants when their barks are wounded [6]. They are materials of high molecular weight, which are soluble in water, or which can be at least dispersed therein. Gum tragacanth is a complex, heterogeneous and anionic carbohydrate with prominent structural stability to heat, acidity and aging [7–9]. This acidic polysaccharide has high molecular weight and it is derived from the bark of 15 different species of Astragalus [10]. GT consists of a linear 1,4 linked α-D-galacturonic acid backbone with three types of side chains: single β-D-xylopyranose and disaccharide units of 2-O-α-L-fucopyranosyl-D-xylopyranose and 2-O-β-D-galactopyranosyl-D-xylopyranose [11]. The main structural units of GT are shown in Fig. 1 [12].

This natural biopolymer is a mixture of two polysaccharides. Tragacanthin, galacturonic acid part of tragacanth which is water soluble and it is a neutral, branched with high molecular weight which gives highly viscous solutions and bassorin, the other part of tragacanth, is a complex of methoxylated acids that is insoluble in water and swells to form a gel or viscous solution [13,14].

The gum tragacanth is considered as generally recognized as safe (GRAS) at the 0.2–1.3% level in food stuffs in the USA since 1961. It is also approved as a food additive in European Union and has the number E413 in the list of additives confirmed by the Scientific Committee for Food of the European Community [15]. This biodegradable and biocompatible biopolymer is not allergenic, mutagenic, teratogenic and carcinogenic with no adverse toxicological effects in non-allergic people [15–17]. Several researchers have reported the application of GT in different fields such as the green synthesis of silver nanoparticles [18], immobilizing agent in viral plaque assay [19], hydrogel membranes [20], dressing for healing of burn wounds [21],

* Corresponding author. Tel.: +98 21 64542680; fax: +98 21 66400245.
E-mail address: hajirb@yahoo.com (S.H. Bahrami).

0928-4931/$ – see front matter © 2013 Elsevier B.V. All rights reserved.
http://dx.doi.org/10.1016/j.msec.2013.08.016

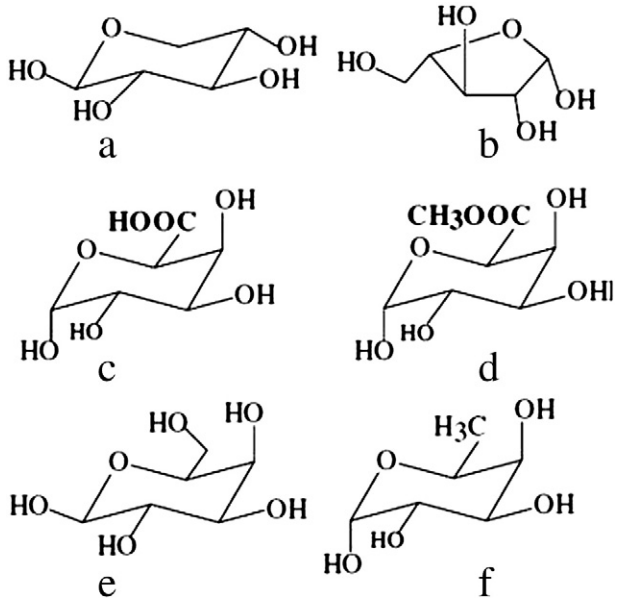

Fig. 1. Main chemical building units of the tragacanth gum. a) β-D-xylose, b) L-arabinose, c) α-D-galacturonic acid, d) α-D-galacturonic acid methylester, e) β-D-galactose, f) α-L-fucose.

super absorbent hydrogel [22] and carrier for controlled release of drugs, etc [23]. Khajavi and coworkers produced GT fibers by solution spinning method via alkaline treatment and they investigated the effects of spinning parameters on the mechanical properties of produced fibers [24,25].

For nanofiber formation, both molecular entanglement and solution viscosity are important [26,27]. Because of high viscosity of GT and its polyonionic behavior [28], production of nanofiber from GT encounters with difficulties and the repulsive interaction among the polyanion along tragacanth chains prevented sufficient chain entanglement which is necessary for fiber formation. Therefore, to reduce repelling interaction and helping electrospinning process in this study hydrophilic PVA which is a non-toxic and biocompatible was blended with GT. Nanofibers were produced from polymer blend solutions of different ratios using electrospinning technique. The effect of blend ratio and electrospinning parameters on the fiber morphology of GT/PVA was studied. Biological evaluation of GT/PVA nanofiber properties such as cytotoxicity and in vitro cell culturing of human fibroblast cell lines AGO provided interesting results indicating that this new biomaterial has the potential of being used in skin regeneration applications.

2. Materials and methods

2.1. Materials

Gum tragacanth used in this study was a high quality ribbon type, collected from the stems of Fluccosus species of Astragalus bushes, growing in central areas of Iran. The raw gum was ground into fine powder. The density and moisture content of GT was 1/42 g/cm3 and 11.4 wt.% respectively. Poly(vinyl alcohol) (Mw = 94–120 kDa) was purchased from MERK, Co. *Staphylococcus aureus* (*S. aureus*) and *Pseudomonas aeruginosa* (*P. aeruginosa*) were used as Gram positive and Gram negative bacteria for microbiological studies. Other chemicals were laboratory grades and they were used without any purification.

2.2. Electrospinning procedures

Known amounts of GT were dissolved in deionized water. After stirring for 8 h, PVA was added to the solutions and agitated for 12 h. The solutions were stored at 4 °C for 6 h to reach the required homogeneity. Blend solutions of GT/PVA were prepared in weight ratios of 0/100, 30/70, 40/60, 50/50, 60/40, 70/30, 100/0 (GT/PVA), in three different concentrations (3, 6 and 9 wt.%). The solutions were fed into a 20 mL plastic syringe fitted with a needle. The feeding rate of the syringe pump changed from 0.5 to 1.5 mL/h. High voltage in the range of 10 to 20 kV was applied using a power supply. GT/PVA electrospun nanofibers were deposited and collected on the collector plate with the distance of 10–20 cm from the needle tip.

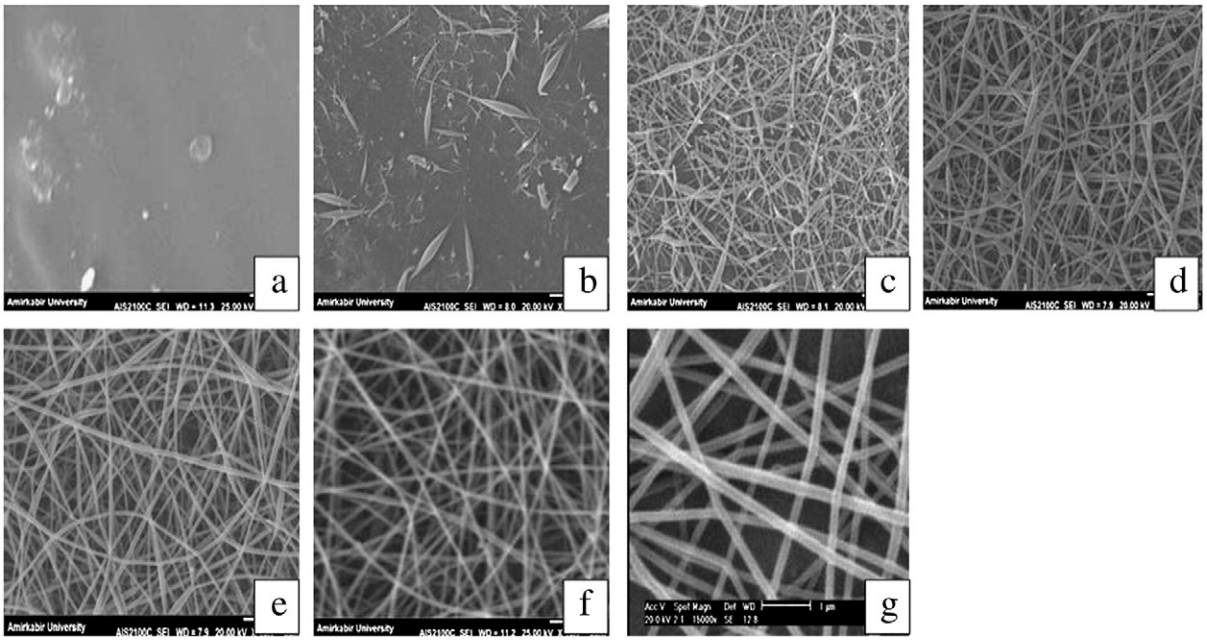

Fig. 2. SEM photographs of nanofibrous web with different weight ratios of GT/PVA: a) 100/0, b) 70/30, c) 60/40, d) 50/50, e) 40/60, f) 30/70, g) 0/100, electrospun at d = 15 cm, V =15 kV, flow rate = 0.5 mL/h 15,000×.

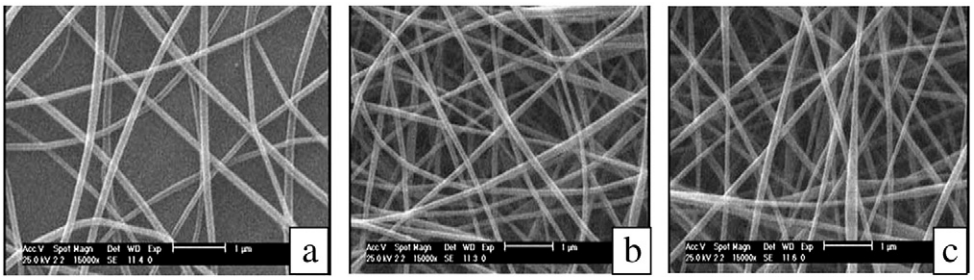

Fig. 3. SEM photographs of nanofibrous mat with different voltages: a) 10 kV, b) 15 kV, c) 20 kV, electrospun at d = 15 cm, flow rate = 0.5 mL/h, solution concentration = 6 wt.%; 15,000×.

Table 1
Diameter of nanofibers produced under different conditions, N = 100.

Feed rate (mL/h)	Concentration (wt.%)	Distance (cm)	Voltage (kV)	Mean fiber diameter (nm)	Std. dev. (%)
0.5	6	15	10	153	16
0.5	6	15	15	140	15
0.5	6	15	20	98	14
0.5	3	15	15	131	31
0.5	9	15	15	210	17
0.5	6	10	15	155	22
0.5	6	20	15	126	17
1.5	6	15	20	134	19
1.5	9	15	15	246	17

The stability and water resistant property of the nanofibers was improved by cross-linking in saturated glutaraldehyde vapors in a desiccator for two days. After crosslinking, the scaffolds were kept in a fume hood overnight and then vacuum dried for three days before using for cell culture and other studies.

2.3. Characterization

The morphology of electrospun GT/PVA bicomponent nanofibers was observed using a scanning electron microscope (SEM) (XL30-SFEG, 12 FEI/Phillips) with gold coating. Fourier transform infrared spectroscopy (FTIR) analysis (Nicolet Magna-IR 560) was used to study the structural changes using KBr method. Thermal properties were examined by differential scanning calorimetry (Universal V3.8B TA Instruments) and samples were heated from room temperature to 250 °C at a heating rate of 10 °C/min in air atmosphere.

2.4. Antimicrobial properties

The agar plate method was used and the antimicrobial behavior of GT/PVA nanofibers and GT solution were examined. In this study *S. aureus* ATCC 25923 and *P. aeruginosa* ATCC 27853 were used as Gram-positive and Gram-negative bacteria respectively. Mueller–Hinton agar media was prepared and sterilized in an autoclave at 121 °C for 20 min under pressure of 103.5 kPa. A loop of each bacterium was inoculated on 5 mL of nutrient broth and incubated at 37 °C for 24 h, then cultured in nutrient agar plate. The disk shape samples of GT/PVA mat were sterilized by ultraviolet light for 2 h and were placed in each plate. Then the plates were held in incubator for 48 h. For testing antibacterial properties of GT solutions, a culture medium filled with 10 mL of 1 wt.% of GT solution was inoculated with test bacteria and cultivated. Photographs from samples were used for assessing the antimicrobial behavior.

2.5. Cell culture

Cell culture tests were carried out for assessing biological compatibility of nanofibers. Human fibroblast cells lines AGO according to ASTM-F813 were cultured in Dulbecco's Modified Eagle Medium (DMEM) supplemented with 15% fetal bovine serum (FBS), 1% antibiotic and antimycotic solutions at 37 °C under a humidified atmosphere of 5% CO_2, 99% relative humidity (RH) and 37 °C. The specimens were sterilized under an ultraviolet lamp for 2 h and soaked with culture medium overnight before cell seeding. A density of 5 × 107 cells/mL was seeded onto electrospun nanofiber and left in incubator for facilitating cell growth. After one day light microscope was used for investigating cell adhesion and cell morphology. The cell-seeded nanofiber was replenished with fresh medium every day. After 2 days of incubation, the scaffold was rinsed twice with phosphate buffer saline (PBS) and subsequently fixed in 2.5% glutaraldehyde for 2 h. After that, the sample was rinsed thrice with PBS for 12 h. Then the sample was immersed in osmium tetroxide 0.1% for 30 min and dehydrated in different concentration of acetone, i.e., 20, 30, 50, 70, 90 and 100% for 10 min each. Finally, the samples were freeze-dried and sputter coated with gold for cell morphology observation by FESEM.

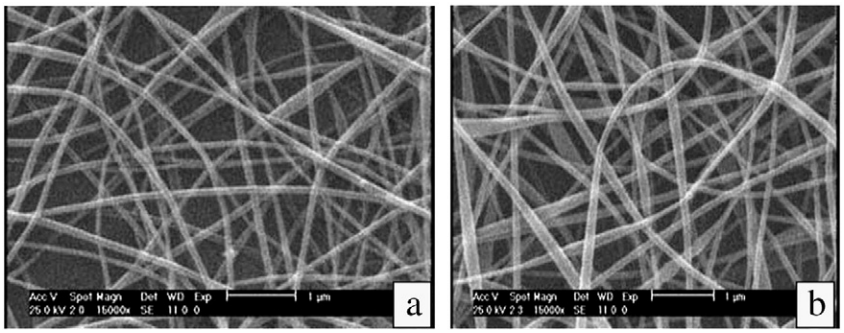

Fig. 4. SEM photographs of nanofibrous mat with different flow rates in constant voltage of 20 kV. a) Flow rate = 0.5 mL/h, b) flow rate = 1.5 mL/h; d = 15 cm, solution concentration = 6 wt.%; 15,000×.

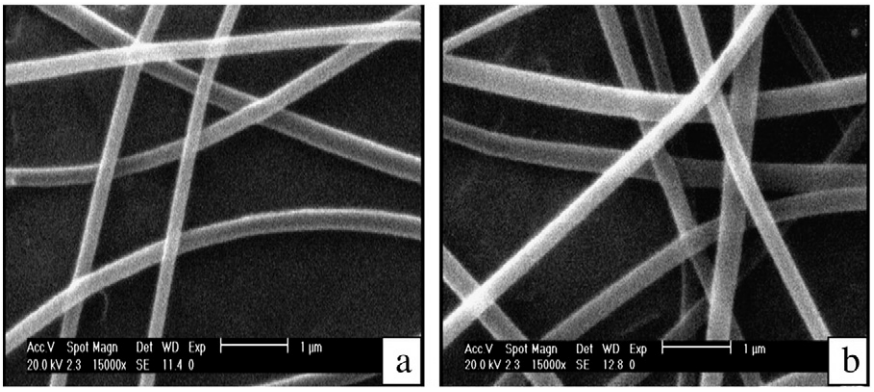

Fig. 5. SEM photographs of nanofibrous mat with different flow rates in constant voltage of 15 kV. a) Flow rate = 0.5 mL/h, b) flow rate = 1.5 mL/h; d = 15 cm, solution concentration = 9 wt.%; 15,000×.

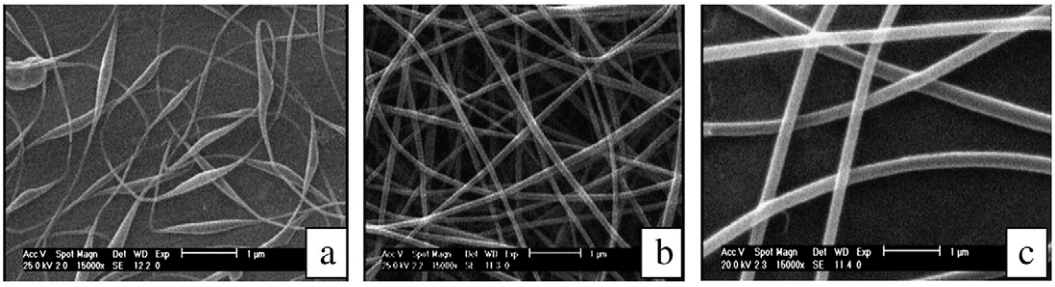

Fig. 6. SEM images of nanofibers with different concentrations. a) 3 wt.%, b) 6 wt.%, c) 9 wt.%, v = 15 kV, d = 15 cm, flow rate = 0.5 mL/h.

2.6. MTT test

This assay is an indirect method for assessing cell growth and proliferation, since mitochondria oxidize the MTT solution, giving a typical blue-violet end product [29]. For MTT test, the proliferation rate of fibroblast cultured scaffolds was compared with the fibroblasts cultured standard plastic substrates. Six samples were prepared for each group. MTT test was performed according to the manufacturer's (Sigma) instructions. After 4 days of cell seeding in 24-well dish, the original medium was removed and 40 μL fresh medium and 50 μL solution of 3-(4,5-dimethylthiazol-2-yl)-2,5-diphenyltetrazolium bromide (MTT) (0.241 mmol) at 1 mg/mL concentration in phosphate-buffered saline (PBS), pH 7.4, was added to 150 μL of sample medium. The MTT component was reduced by mitochondrial dehydrogenase of metabolizing cells, to purple formazan. After 4 hour incubation at 37 C in 5% CO_2 MTT solution from each well was carefully removed and replaced by 250 μL dimethyl sulfoxide. Then the absorbance of solution was measured at 570 nm wavelength (reference wavelength 630 nm) using an ELISA reader. The quantity of formazan product which is measured by the absorbance at 570 nm was directly proportional to the number of viable cells in the culture. A statistical analysis between control sample (tissue culture plate TCP) and GT/PVA nanofiber was performed using the nonparametric Mann–Whitney U test ($P < .05$).

2.7. Statistical analysis

All data were presented as mean ± standard deviation (SD). The statistical significance of the obtained data was analyzed by nonparametric Mann–Whitney U-test for MTT results. Probability values of $P < 0.05$ were interpreted as denoting statistical significance.

3. Results and discussion

3.1. Effect of blend ratio on nanofiber morphology

GT solution (2 wt.%) was kept in the syringe and extruded at 0.5 mL/h under 15 kV voltage and 15 cm distance from collector. Due to charge repulsion among the polyanions along the GT chains

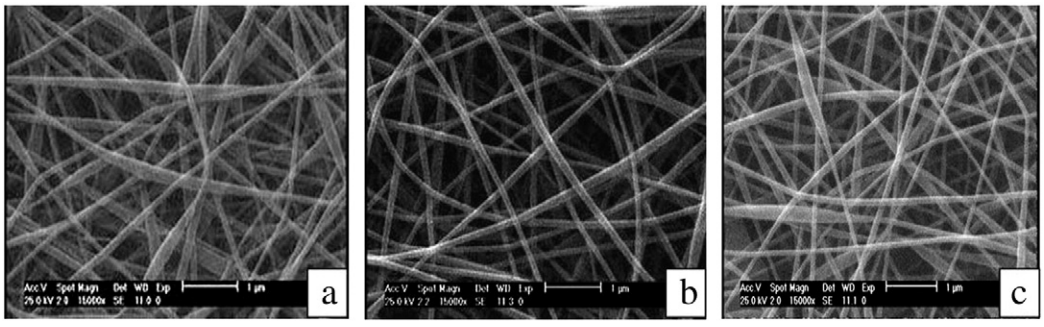

Fig. 7. SEM images of nanofibers with different distances. a) 10 cm, b) 15 cm, c) 20 cm, 6 wt.%, v = 15 kV, flow rate = 0.5 mL/h.

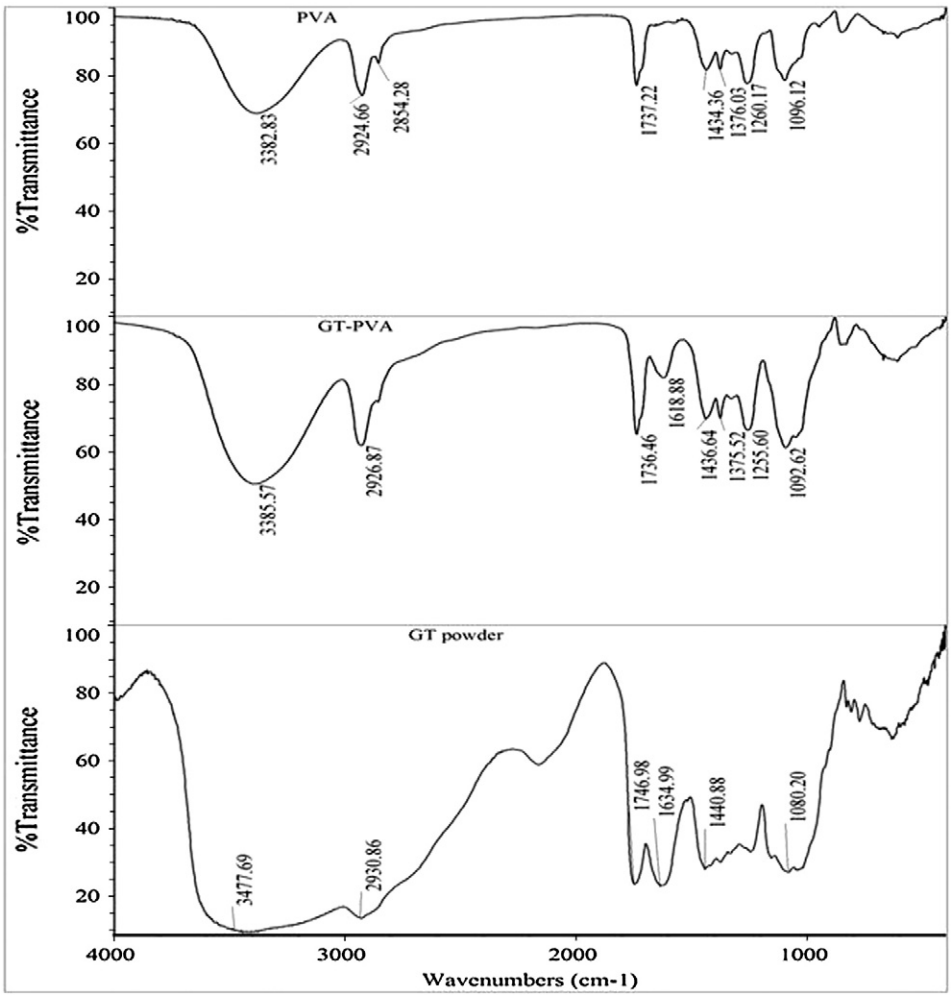

Fig. 8. FTIR spectra, PVA nanofiber, GT powder, GT/PVA.

which results in lack of chain entanglements and high viscosity of solution due to high molecular weight, this polymer could not form nanofibers and collected on the collector surface in the form of scattered droplets (Fig. 2a). Therefore, PVA was used to mitigate the charge repulsions between polyanion GT molecules and to enhance the molecular entanglement [30].

GT/PVA blend solutions with different blend ratio were prepared. By blending GT with poly(vinyl alcohol) (PVA), nanofibers could be obtained. Since GT is slightly acidic polysaccharide, the morphology and diameter of electrospun nanofibers would be critically influenced by the weight ratio of GT/PVA. In PVA/GT blends, presence of PVA resulted in reducing the repulsive forces at 70/30 wt.% (GT/PVA) and the shape of the beads changed from spherical to spindle like (Fig. 2b). When the amount of PVA in the blend increased to 40%, these random spindle shape were more like broken fibers (Fig. 2c) and with further increase in amount of PVA to 50%, nanofibers with uneven diameters were formed (Fig. 2d). When the PVA content increased to 60% and 70% in the blend solution, uniform, beadles and crackles nanofibers could be obtained (Fig. 2e and f). However, GT/PVA with the blend ratio of 40/60 wt.% was selected as optimum blend ratio because of having higher amount of GT.

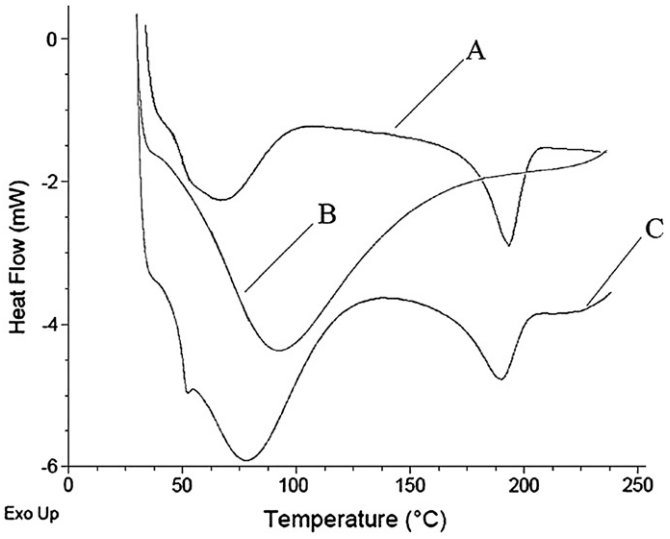

Fig. 9. DSC curves of the samples; A) PVA nanofibers, B) GT powder, C) GT/PVA nanofiber.

3.2. Effect of voltage

To investigate the effect of instability on the apex of the syringe needle where the electrospinning jet originates, a series of experiments were carried out in which the applied voltage varied from 10 to 20 kV, with constant feeding rate 0.5 mL/h and tip-target distance of 15 cm. SEM images of nanofibers obtained are shown in Fig. 3a–c. As it can be seen from these figures, with increasing the voltage from 10 to 20 kV, the ejected jet gets affected by higher electric field so that the jet gets more and more extended in its path from the nozzle to the collector

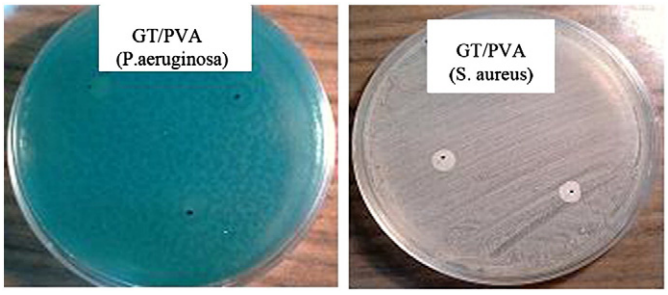

Fig. 10. Bactericidal activity of GT/PVA nanofibrous mat with Gram positive *Staphylococcus aureus* and Gram-negative *P. aeruginosa*.

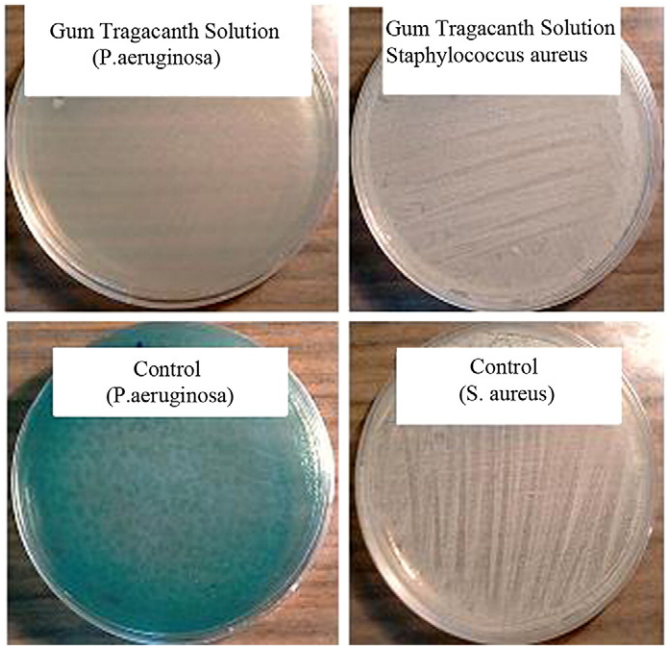

Fig. 11. Bactericidal activity of GT solution with Gram-positive *S. aureus* and Gram-negative *P. aeruginosa*.

and fiber diameter decreases from 153 to 98 nm and uniformity of the formed nanofibers increases (Table 1). Applied voltage plays a critical role in the electrospinning process and provides the surface charge on the electrospinning jet. A higher voltage will lead to greater stretching of the solution due to the greater columbic forces in the jet as well as the stronger electric field [31,32].

3.3. Effect of feed rate

A certain minimum value of the solution should be maintained at the tip of the needle in order to form an equilibrium Taylor cone [33]. Therefore, different morphologies of electrospun nanofibers can be obtained with the change in feeding rates at a given voltage. This parameter of electrospinning process has different effect on nanofibers with different polymer [34]. To investigate the effect of feed rate on the diameter of nanofibers, some experiments were carried out in which the feed rate was varied from 0.5 to 1.5 mL/h, with constant applied voltage 20 kV and tip-target distance of 15 cm and solution concentration of 6 wt.%, respectively. It was observed that with increasing the extrusion rate, the diameter of nanofibers increases and uniformity was decreased (Fig. 4a,b, Table 1). This is because when higher amount of polymer solution is extruded from tip of the needle it will have higher amount of solid polymer in it which has to be solidified during same time period (distance being the same) while, same amount of electric charges is applied on the solution stream. This will result in increasing the fiber diameters with increasing the extrusion rate [1]. At voltage of 15 kV, tip-target distance of 15 cm and solution concentration of 9 wt.%, with increasing feed rate from o.5 to 1.5 mL/h the same behavior could be observed (Fig. 5a,b, Table 1).

3.4. Effect of concentration

Polymer concentration has a great influence on the electrospinning process and it affects surface tension of the solution [35]. The relationship between the polymer viscosity and/or concentration on fibers obtained from electrospinning has been studied in many articles [36,37]. The polymer concentration must be high enough to cause polymer entanglements and do not prevent the polymer flow when subjected to an electrical field. Low concentration of solution results in many beads or many microspheres and when the concentration became low enough, the process might change to electrospraying. Fig. 6 shows that when the concentration was 3%, there were stretched spindle like fibers collected on the collector plate (Fig. 6a). However, when the concentration increased to 6 wt.%, smooth surface nanofibers with high uniformity were produced (Fig. 6b) and with further increasing the concentration from 6 wt.% to 9 wt.%, there was a considerable increase in the viscosity which affected the electrospinning. This high viscosity prevented the electric field and the current present in the field could not stretch the solution jet therefore, the diameter of the nanofibers increased from 140 nm to 210 nm and subsequently lesser number of nanofibers were collected on the collector (Fig. 6c, Table 1). Other spinning parameters were kept constant at 15 cm distance, 0.5 mL/h extrusion rate.

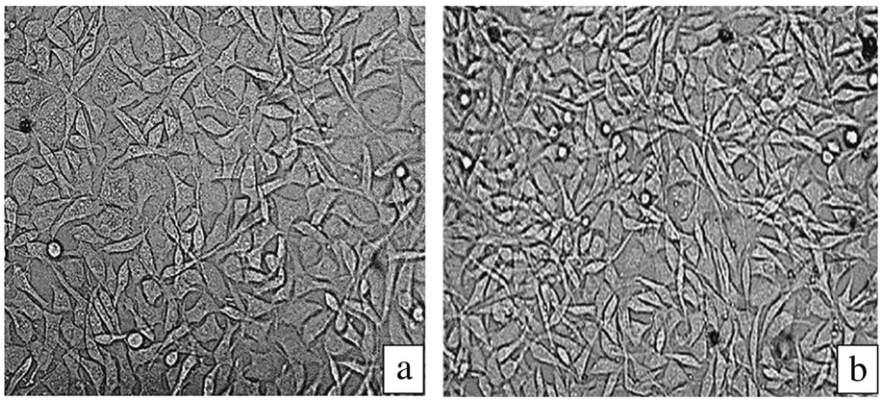

Fig. 12. Adhesion of human fibroblast cell lines AGO on: a) control sample, b) electrospun GT/VA nanofiber (light microscopy, scale bars: 40 μm).

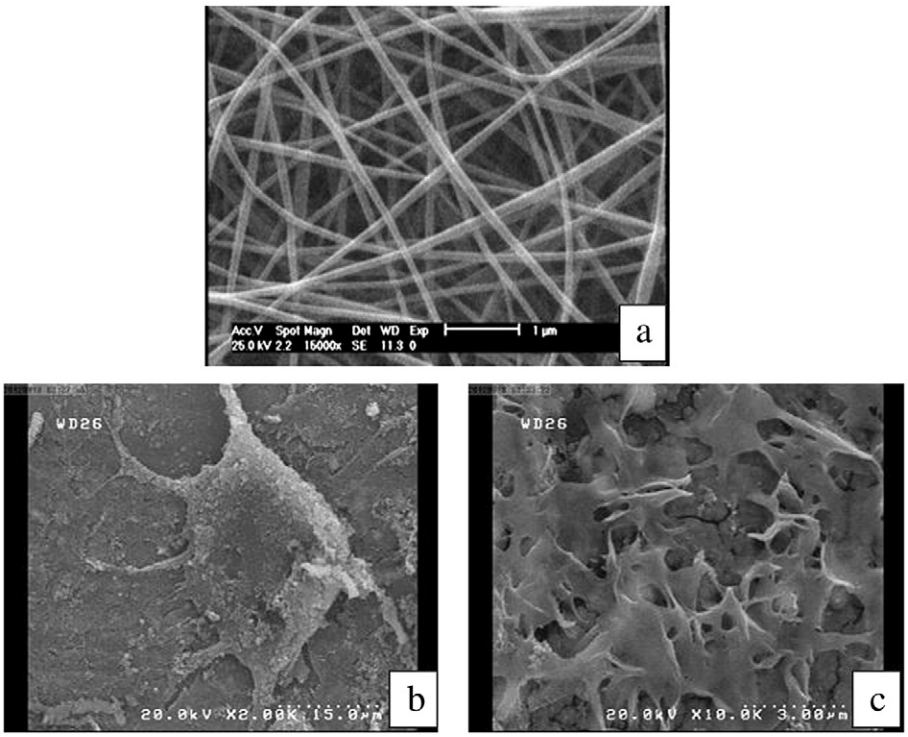

Fig. 13. SEM micrographs of a) electrospun nanofibers, b, c) fibroblast electrospun GT/PVA nanofibers in different magnifications.

3.5. Effect of distance between tip and collector

Varying the distance between the tip of nozzle and the collector has been examined to control the fiber diameters and morphology. It will have a direct influence in both the flight time and the electric field strength. A minimum distance is required to provide sufficient time for drying the fibers before reaching the collector. When the distance between nozzle and collector is either too short or too long, nanofibers with beads will form [38]. Increasing the distance between tip and collector, decreases the average fiber diameter. However, there are cases where at a longer distance, the fiber diameter increases in the case of PVA [39]. Therefore, in GT/PVA nanofibers it seems that increasing the distance between tip and collector from 10 cm to 20 cm, decreases fiber diameter and nanofibers with more surface uniformity were obtained (Fig. 7).

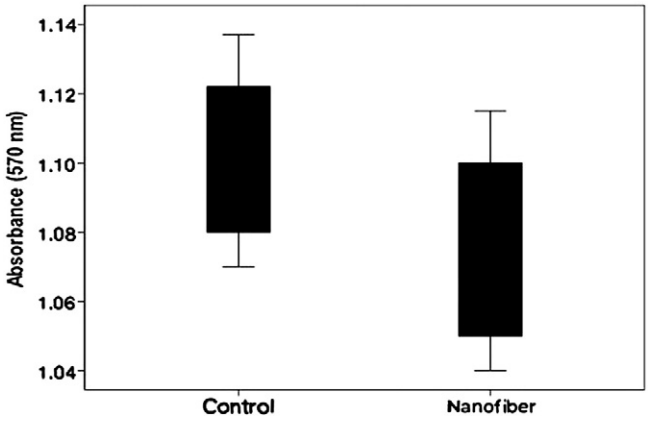

Fig. 14. Box plot graphs of MTT results of fibroblast on nanofiber web in 3 days. Data were analyzed by the non-parametric method of the Mann–Whitney U test, $P < 0.05$.

3.6. FTIR result

FTIR spectra of GT powder, PVA and GT/PVA nanofibers were recorded (Fig. 8). The major absorbance bands present in the spectra of GT were at 3442, 2930, 2856, 2158, 1747, 1635, 1441, 1367, 1243, 1080 and 1023 cm^{-1}. The broad band observed at 3442 cm^{-1} could be assigned to stretching vibrations of O–H groups in the gum tragacanth. The bands at 2930 and 2856 cm^{-1} correspond to asymmetric and symmetric stretching vibrations of methylene groups and the broad band at 2158 cm^{-1} shows various carbonyl species of the gum. The sharp peak at 1747 cm^{-1} could be assigned to carbonyl stretching vibrations in aldehydes, ketones and carboxylic acids. The stronger band found at 1635 cm^{-1} could be assigned to characteristic asymmetrical stretch of carboxylate group. Bands at 1441 and 1367 cm^{-1} could be attributed to symmetrical stretch of carboxylate groups and bands at 1441 and 1367 cm^{-1} showed the symmetrical stretch of carboxylate group. The peaks at 1243 cm^{-1} and 1143 cm^{-1}; 1080 cm^{-1} and 1023 cm^{-1} were due to the C–O stretching vibrations of polyols, ether and alcoholic groups, respectively. The spectra of PVA (Fig. 8) indicated an intense band due to the presence of hydroxyl groups (O–H) at 3382 cm^{-1}. The bands corresponding to the ($-CH_2-$) asymmetric and the symmetric stretching could be seen at 2925 cm^{-1} and 2854 cm^{-1}. The band at 1737 and 1434 cm^{-1} can be attributed to carbonyl stretching vibrations; O–H and C–H bending respectively. The FTIR spectra of GT/PVA blend nanofibers showed the characteristic peaks of GT and PVA such as 1637 cm^{-1} which is attributed to asymmetrical stretch of carboxylate group. This peak which appeared at 1635 cm^{-1} for GT shifted to lower frequency in GT/PVA nanofiber and appeared at 1618 cm^{-1}. It is also observed that the bands for hydroxyl

Table 2
MTT results for GT/PVA nanofibers.

Fibroblasts on	Number of samples	Colorimetric reading average OD (±SD)	P value
GT/PVA nanofiber	6	1.072 (±0.027)	>0.05
Control	6	1.097 (±0.024)	

stretching become much broader with adding GT. This may be due to presence of hydrogen bonding between OH groups of PVA and −COO or OH group of GT [40,41].

3.7. DSC result

DSC thermogram of the GT powder, PVA and GT/PVA nanofibers are shown in Fig. 9. In PVA there are two exothermic peaks. The first peak is assigned to moisture evaporation from the sample and the T_g appears at 62 °C. Another peak at 194 °C is due to the melting of PVA [42–44]. This exothermic peak starts from 165 °C and finishes at 200 °C (Fig. 9A). On the other hand GT shows a very broad exothermic peak starting from 50 °C and ending at 158 °C with the peak temperature at 89 °C. This peak is corresponding to the hydrophilic nature of functional groups of GT and appears due to dehydration of GT. Gum tragacanth started to decompose slowly at 250–280 °C (Fig. 9B) [8]. In the blend nanofiber, the peak due to dehydration shifts to 78 °C, which falls between two dehydration peaks of PVA and GT. This peak starts from 50 °C and finishes at 123 °C. The melting peak of PVA shifts to slightly lower temperature starting at 162 °C and ending 201 °C. This shows presence of GT affected the thermal behavior of PVA (Fig. 9C).

3.8. Antibacterial properties

Antibacterial activity of GT/PVA nanofibers was investigated using disk shape webs. The samples showed the antibacterial property against Gram-negative bacteria (*P. aeruginosa*) and the zone of inhibitory was visible in the plate (Fig. 10). This bacterium has very bad effect on the wound when the skin gets injured [45]. But there was no clear zone around the sample in the plate containing Gram-positive bacteria (*S. aureus*). Since GT could not be converted into nanofibers, to investigate the effect of GT on antibacterial properties of the blend fibers, *P. aeruginosa* was cultured in the plate of containing GT solution. As it can be seen from Fig. 11, GT solution protected from growth of Gram negative bacteria and blue-green pigment is not visible. Possibly the L-sugars found in tragacanth (L-arabinose and L-fucose) are responsible for the extraordinary resistance to microbial attack, since most organism would be unable to metabolize these foreign sugars [46].

3.9. Cell culture

Cells in their growing process pass through four stages, at first stage cells have spherical shapes which later at second stage develop some false feet. At third stage the false feet grow and adhesion of cells takes place, and finally at the last stage flatting of cells occurs. In last step, they have very good viability in the medium. If the number of flatted cells is more than the number of spherical cells, it is an indication for a good compatibility in the medium expose to the material. The results of Fig. 12 showed excellent cell viability in this medium when the cells were exposed to GT/PVA nanofibers for 1 day in CO_2 incubator, 99% RH and 37 °C. The attachment of cells on the nanofiber scaffold is similar to that of the tissue culture plate and most of the cells grow well and get a flat shape which is an indication of a very good compatibility with the blend GT-PVA nanofiber samples. Cell morphology and the interaction between cells and nanofibers were studied after 2 days of cell culture by SEM. Fig. 13 shows the fibroblast attachment and growth on GT/PVA electrospun nanofiber after cell fixation. It can be seen that fibroblast cells adhered and spread on the surface of the polymer nanofiber and these cells interacted and integrated well with the surrounding fibers.

3.10. MTT assay

In order to show cell adhesion and proliferation of GT/PVA nanofiber, the number of cells was determined using the colorimetric MTT assay. The results of MTT test are summarized in Fig. 14. If P-value* is more than 0.05 it indicates that there is no significant difference between the scaffold and its positive control. Therefore, these scaffolds enhance the cell infiltration well and are proper to be selected for other biological investigation such as in vivo tests. MTT assay showed that for GT/PVA nanofiber, P-value* is more than 0.05 (Table 2) therefore this scaffold is suitable for tissue engineering applications.

4. Conclusions

Due to repulsive interaction among the polyanions along the GT chains and high viscosity of solutions, GT could not be electrospun. To improve the spinnability of GT, poly(vinyl alcohol) was blended with this polysaccharide. The results showed that, it is possible to produce smooth surface nanofibers without any beads. The ratio of GT/PVA varied and nanofibers with best morphology were obtained at 40/60 GT/PVA ratios. The average diameter of nanofibers increased with changing solution concentration from 3% to 9 wt.%, feed rate from 0.5 to 1.5 mL/h, applied voltage from 20 to 10 kV and electrode spacing distance from 20 to 10 cm. The FTIR spectra of GT/PVA blend nanofibers showed the characteristic peaks of GT and PVA. The sample showed good antimicrobial property against Gram-negative bacteria (*P. aeruginosa*). Human fibroblast lines AGO had well attachment and proliferation on the GT/PVA nanofiber scaffolds. MTT assay confirmed nanofibers have cell viability property and biological compatibility. Biocompatibility and antibacterial properties of nanofibers showed that these nanofibers are effective wound dressing and these nanofibers can protect the wound area from its surroundings to avoid infection and dehydration and speeding up the healing process by providing an optimum microenvironment for healing, removing any excess wound exudates, and allowing continuous tissue reconstruction.

Acknowledgment

The authors wish to thank the Center for Excellence Modern Textile Characterization, Tehran Iran for their support in providing the means for conducting the experiments.

References

[1] S. Agarwal, J.H. Wendorff, A. Greiner, Adv. Mater. 21 (2009) 3343–3351.
[2] Q.P. Pham, U.A. Sharma, A.G. Mikos, Tissue Eng. 12 (2006) 1197–1211.
[3] A. Martins, J.V. Araújo, R.L. Reis, N.M. Neves, Nanomedicine 2 (2007) 929–942.
[4] Z.X. Meng, Y.S. Wang, C. Ma, W. Zheng, L. Li, Y.F. Zheng, Mater. Sci. Eng. C 30 (2010) 1204–1210.
[5] H. Homayoni, S.A.H. Ravandi, M. Valizadeh, Carbohydr. Polym. 77 (2009) 656–661.
[6] S. Balaghi, M.A. Mohammadifar, A. Zargaraan, Food Biophysics 5 (2010) 59–71.
[7] N. Gralen, M. Karhholm, Colloid.sci. 5 (1950) 21–36.
[8] M.J. Zohuriaan, F. Shokrolahi, Polym. Test. 23 (2004) 575–579.
[9] S. Balaghi, M.A. Mohammadifar, A. Zargaraan, Food Hydrocolloids 25 (2011) 1775–1784.
[10] D. Verbeken, S. Dierckx, K. Dewettinck, Appl. Microbiol. Biotechnol. 63 (2003) 10–21.
[11] A. Yokoyama, K.R. Srinivasan, H.S. Fogler, J. Colloid Interface Sci. 126 (1988) 141–149.
[12] Z. Mohamadnia, M.J. Zohuriaan-Mehr, K. Kabiri, M. Razavi-Nouri, Polym. Res. 15 (2008) 173–180.
[13] M.A. Mohammadifar, S.M. Musavi, A. Kiumarsi, P.A. Williams, Int. J. Biol. Macromol. 38 (2006) 31–39.
[14] C.A. Tischer, M. Iacomini, P.A.J. Gorin, Carbohydr. Res. 337 (2002) 1647–1655.
[15] G.O. Phillips, P.A. Williams, second ed., Woodhead Publishing Limited, Cambridge, UK, 2009.
[16] D.M.W. Anderson, Food Addit. Contam. 6 (1989) 1–12.
[17] M.A. Eastwood, W.G. Brydon, D.M.W. Anderson, Toxicol. Lett. 21 (1984) 73–81.
[18] A.J. Kora, J. Arunachalam, Nanomater. (2012) 1–8(Article ID 869765).
[19] J. O'Mahony, M. O'Donoghue, J.G. Morgan, C. Hill, Int. J. Food Microbiol. 61 (2000) 177–185.
[20] A. Kiani, M. Shahbazi, H. Asempour, J. Appl. Polym. Sci. 124 (2012) 99–108.
[21] A. Moghbel, H. Agheli, E. Kalantari, M. Naji, J. Toxicol. Lett. 18 (Supplement 1) (2008) S154.
[22] F. Khoylou, F. Naimian, Radiat. Phys. Chem. 78 (2009) 195–198.
[23] M.R. Siahi, M. Barzegar-Jalali, F. Monajjemzadeh, F. Ghaffari, S. Azarmi, AAPS Pharm. Sci. Tech. 6 (2005) E626–E632.
[24] R. Khajavi, S.H.M. Pourgharbi, A. Rashidi, A. Kiumarsi, Int. J. Eng. 17 (2004) 201–208.

[25] R. Khajavi, S.H.M. Pourgharbi, A. Kiumarsi, A. Rashidi, Appl. Sci. 7 (2007) 2861–2865.
[26] K.Y. Lee, L. Jeong, Y.O. Kang, S.J. Lee, W.H. Park, Adv. Drug Deliv. Rev. 61 (2009) 1020–1032.
[27] L. Li, Y.L. Hsieh, Polymer 46 (2005) 5133–5139.
[28] A. Yokoyama, K.R. Srinivasan, H.S. Fogler, Colloid Interface Sci. 126 (1988) 141–149.
[29] C. Tonello, B. Zavan, R. Cortivo, P. Brun, S. Panfilo, G. Abatangelo, Biomaterials 24 (2003) 1205–1211.
[30] S.I. Jeong, M.D. Krebs, C.A. Bonino, S.A. Khan, E. Alsberg, Macromol. Biosci. 10 (2010) 934–943.
[31] C.J. Buchko, L.C. Chen, Y. Shen, D.C. Martin, Polymer 40 (1999) 7397–7407.
[32] S. Megelski, J.S. Stephens, D.B. Chase, J.F. Rabolt, Macromolecules 35 (2002) 8456–8466.
[33] S. Ramakrishna. in: N.J. Hackensack (Eds.), World Scientific, Singapore, 2005.
[34] X.H. Zhong, K.S. Kim, D.F. Fang, S.F. Ran, B.S. Hsiao, B. Chu, Polymer 43 (2002) 4403–4412.
[35] K.H. Lee, H.Y. Kim, H.J. Bang, Y.H. Jung, S.G. Lee, Polymer 44 (2003) 4029–4034.
[36] H.S. Kim, K. Kim, H.J. Jin, I.J. Chin, Macromol. Symp. 224 (2005) 145–154.
[37] J.M. Deitzel, J. Kleinmeyer, D. Harris, N.C.B. Tan, Polymer 42 (2001) 261–272.
[38] T. Jarusuwannapoom, W. Hongrojjanawiwat, S. Jitjaicham, L. Wannatong, M. Nithitanakul, C. Pattamaprom, P. Koombhongse, R. Rangkupan, P. Supaphol, Eur. Polym. 41 (2005) 409–421.
[39] J.S. Lee, K.H. Choi, H.D. Ghim, S.S. Kim, D.H. Chun, H.Y. Kim, W.S. Lyoo, Appl. Polym. Sci. 93 (2004) 1638–1646.
[40] T. Çaykara, S. Demirci, J. Macromol. Sci. A 43 (2006) 1113–1121.
[41] S. Safi, M. Morshed, S.A. Hosseini Ravandi, M. Ghiaci, J. Appl. Polym. Sci. 104 (2007) 3245–3255.
[42] N.A. El-Zaher, W.G. Osiris, J. Appl. Polym. Sci. 96 (2005) 1914–1923.
[43] N.A. Peppas, E.W. Merrill, J. Appl. Polym. Sci. 20 (1976) 1457–1465.
[44] E. Parparita, C.N. Cheaburu, C. Vasile, Cellul. Chem. Technol. 46 (2012) 571–581.
[45] J.A. Driscoll, S.L. Brody, M.H. Kollef, Drugs 67 (2007) 351–368.
[46] R.L. Davidson, McGraw-Hill Book Company., New York. 1980, chapter 11.